Origin of anomalous line shape of the lowest-frequency $A_1(\mathrm{TO})$ phonon in $PbTiO_3$

Seong M. Cho, Hyun M. Jang,* and Tae-Yong Kim
Department of Materials Science and Engineering and National Research Laboratory (NRL) for Ferroelectric Phase Transitions, Pohang University of Science and Technology (POSTECH), Pohang 790-784, Korea

(Received 8 September 2000; revised manuscript received 18 January 2001; published 12 June 2001)

The origin of the anomalous line shape of the $A_1(1\mathrm{TO})$ soft mode in $PbTiO_3$-based single crystals was investigated by polarized Raman-scattering method over a wide range of temperature between 100 and 700 K. Detailed scattering data indicated that the previously proposed anharmonicity model could not properly explain the anomalous behavior of the lowest-frequency subpeak of the $A_1(1\mathrm{TO})$ mode that was primarily responsible for the phonon softening of the undoped $PbTiO_3$. Further Raman studies of Ba-doped $PbTiO_3$ crystals showed that the Ba-impurity peak that dominated the soft-mode transition also had the A_1 symmetry of the $PbTiO_3$ host lattice. A careful comparison of these two distinct peaks having the same A_1 symmetry indicates that the observed anomalous line shape of the $A_1(1\mathrm{TO})$ mode is caused not only by the lattice anharmonicity but also by some lattice defects. Particularly, the lowest-frequency subpeak of the $A_1(1\mathrm{TO})$ mode is not directly related to the anharmonicity but originates from the existence of thermodynamically unavoidable lattice defects in $PbTiO_3$.

DOI: 10.1103/PhysRevB.64.014103 PACS number(s): 77.80.Bh, 77.84.Dy, 78.30.−j, 63.20.−e

I. INTRODUCTION

Lead titanate ($PbTiO_3$) has been widely studied[1–21] during last few decades because of its importance in science and technology. It has relatively a simple structure among many perovskite-based ferroelectrics and shows a typical displacive transition character. Therefore, lead titanate has been regarded as a model system for the study of displacive ferroelectric transitions. In addition, it is an important constituent of lead-based complex perovskites [e.g., $Pb(Zr,Ti)O_3$; PZT] that are extremely important in modern electronic technology.

Lead titanate undergoes a cubic-to-tetragonal phase transition at 763 K.[1] Although there exist some controversial arguments over the nature of phase transition (i.e., displacive versus order-disorder transition),[2–5] $PbTiO_3$ has long been regarded as a typical ferroelectric system that undergoes a displacive transition with underdamped soft phonons.[6] These soft modes have been studied by Raman scattering[1,7–11] and neutron scattering.[12]

The first detailed study on the Raman scattering of single-crystal $PbTiO_3$ was made by Burns and Scott.[1,7] They had assigned all the Raman active modes of tetragonal perovskite $PbTiO_3$ and observed the softening behavior of the lowest-frequency E-symmetry transverse-optical $[E(1\mathrm{TO})]$ phonon that drives a displacive ferroelectric phase transition. However, the lowest-frequency A_1-symmetry transverse-optical $[A_1(1\mathrm{TO})]$ phonon could not be directly observed. They determined the frequency of this mode by fitting the angular dependence of the oblique phonon spectra (with $\mathbf{k}$ at 45° between a and c axis) using Merten's relation. This fitting demonstrated the expected soft-mode behavior of the $A_1(1\mathrm{TO})$ phonon.

The first mode assignment of the $A_1(1\mathrm{TO})$ phonon was suggested by Fontana and co-workers.[8] They assigned the anisotropic peak located around 148 cm^{-1} as the $A_1(1\mathrm{TO})$ phonon because it rigorously follows the selection rules of Raman scattering. However, they did not give any explanation for the asymmetry of its line shape.

The first explanation for the complex line shape of the $A_1(1\mathrm{TO})$ mode was given by Foster and co-workers.[9,10] They reported the direct observation of all Raman active phonons of $PbTiO_3$ including the $A_1(1\mathrm{TO})$ mode phonon. Their assignment of the $A_1(1\mathrm{TO})$ mode was the same as that of Fontana *et al.*[8] They attributed the anomalous line shape of the $A_1(1\mathrm{TO})$ mode to the anharmonic nature of the effective interatomic potential.[9,10] Their assignment of the $A_1(1\mathrm{TO})$ mode, however, is different from that of Burns and Scott.[1,7] According to the assignment of Foster and co-workers, the energy of the $A_1(1\mathrm{TO})$ mode is higher than that of the lowest-frequency E-symmetry longitudinal-optical $[E(1\mathrm{LO})]$ mode at room temperature. Since the $A_1(1\mathrm{TO})$ mode is the soft mode, these two $\mathbf{k}\approx 0$ modes should cross at elevated temperatures. However, their study was restricted to 400 K, and, thus, the high-temperature behavior of the $A_1(1\mathrm{TO})$ phonon could not be observed.

Recently, the high-temperature behavior of the $A_1(1\mathrm{TO})$ phonon of single-crystal $PbTiO_3$ was examined by Cho and Jang.[11] They observed the mode crossing between the $A_1(1\mathrm{TO})$ phonon and the $E(1\mathrm{LO})$ phonon and the softening behavior of the $A_1(1\mathrm{TO})$ mode directly. The observed crossing behavior clearly supported the assignment of the $A_1(1\mathrm{TO})$ and $E(1\mathrm{LO})$ modes that had been originally suggested by Foster and co-workers.[9,10] However, the high-temperature behavior (for $T>400$ K) of the $A_1(1\mathrm{TO})$ phonon[11] strongly deviated from the anharmonicity model proposed by Foster *et al.*[9,10] Therefore, further systematic study is needed to clarify the origin of this anomalous behavior of the $A_1(1\mathrm{TO})$ soft mode that is primarily responsible for the cubic-tetragonal displacive transition.

In this study, we have systematically investigated the origin of the anomalous line shape of the $A_1(1\mathrm{TO})$ phonon at a high-temperature region ($T\geqslant 400$ K) by reexamining the anharmonicity model and by carefully comparing the impurity vibration mode of Ba-doped $PbTiO_3$ crystals with the

lowest-frequency subpeak of the $A_1(1TO)$ mode of pure $PbTiO_3$. It is concluded that the lowest-frequency subpeak of the $A_1(1TO)$ mode that dominates the phonon softening of the undoped $PbTiO_3$ is not related to the anharmonicity in the normal mode vibration but originates from some thermodynamically unavoidable lattice defects.

II. EXPERIMENTAL

Pure and Ba-doped $PbTiO_3$ single crystals used in this study were grown by the PbO flux method.[22] The flux composition was 80 at.% PbO-20 at.% TiO_2, and a small amount of $BaCO_3$ was added to the starting flux for the growth of Ba-doped crystals. Regardless of the Ba content, the temperature range of the growth was between 1343 and 1173 K. The cooling rate was 1 K/hr. The Ba contents of the grown crystals were evaluated using the inductively coupled plasma (ICP) wet chemical analysis. Both pure $PbTiO_3$ and 0.7, 1.3, 3.8 at.% Ba-doped single crystals were successfully grown using this flux method.

Both undoped and Ba-doped single crystals had bright yellow color and were platelet in their shape with final dimensions of about $2\text{mm}\times 3\text{mm}\times 1\text{mm}$. Crystallographic directions of the grown crystal were determined by x-ray diffraction. The plate face of the grown crystal corresponded to the (001) plane of the tetragonal structure, and the other faces were (100)-family planes. In addition, as-grown crystals had a few twins and natural 90° domains at edge regions but they were not poled. Since the spatial resolution of the present Raman system was sufficiently high ($\sim 50\ \mu$m), a single-domain spectrum could be readily obtained without the polarization leakage caused by 90° domains even using unpoled crystals.

Raman-scattering data were obtained using a NRS2100 Raman spectrometer (JASCO, Japan) that adapted a triple monochromator. A Coherent Innova 90C Ar laser operating at 5145 Å was used as a light source. The spectral resolution was 1 cm^{-1}. For measurements over a wide range of temperature, a temperature control system supplied by MMR Tech. (U.S.A.) was employed.

III. RESULTS AND DISCUSSION

A. $A_1(1TO)$ mode of pure $PbTiO_3$ crystal

Figure 1 shows the polarized Raman spectra of the $A_1(1TO)$ mode of the pure single-crystal $PbTiO_3$ at various temperatures ranging from 300 to 700 K. All the spectra were obtained in $x(zz)x$ backscattering geometry and were normalized with their integrated peak areas. From Fig. 1, it is apparent that the $A_1(1TO)$ mode has a complex line shape, composed of four subpeaks. The origin of this anomalous line shape of the $A_1(1TO)$ mode was explained earlier by Foster *et al.*[9,10] They advocated that $A_1(1TO)$ mode had a double-well potential in the ferroelectric state and the anharmonicity of the double-well potential was the origin of the observed subpeak structure for temperatures up to 400 K. According to this anharmonicity model, the $A_1(1TO)$ mode consists of four distinct subpeaks, and each subpeak corresponds to the vibrational transition from one quantum state

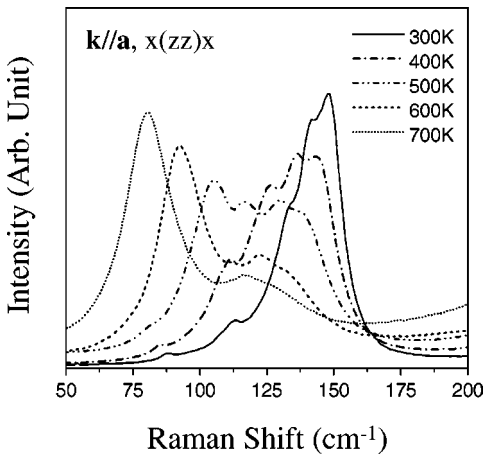

FIG. 1. The temperature dependence of Raman spectra for the $A_1(1TO)$ mode of the pure $PbTiO_3$ single crystal. All the spectra were obtained in $x(zz)x$ backscattering geometry.

to its neighboring quantum state. Therefore, the first subpeak that has the highest frequency among the four subpeaks corresponds to the transition from $n=0$ to $n=1$ in the vibrational quantum states. Similarly, second, third, and fourth subpeaks, respectively, correspond to the transition from $n=1$ to $n=2$, from $n=2$ to $n=3$, and from $n=3$ to $n=4$ in the vibrational states. This labeling of the A_1 subpeaks is in contrast with our previous labeling.[11] However, we believe that this new labeling gives a better readability with less confusion.

Foster and co-workers[9,10] used the following relation to theoretically estimate the relative intensity R of the transition (Stokes) from level n to $n+1$ to that from level 0 to 1:

$$R=(n+1)\exp\left(\frac{-n\hbar\omega}{k_BT}\right), \tag{3.1}$$

where k_B is Boltzmann's constants, and ω is the phonon frequency in the vibrationally ground state. Using Eq. (3.1), they successfully analyzed the intensities of the $A_1(1TO)$ phonon up to 400 K. Following this study, *ab initio* computational results in the mean-field approximation were presented.[15,16] However, there were some discrepancies between the experimentally obtained intensities and the computational results for the $A_1(1TO)$ subpeaks.

The most prominent feature of Fig. 1 is a strong intensity transfer toward the lowest-frequency subpeak above 400 K. Thus, the high-temperature line shape of the $A_1(1TO)$ mode is dominated by the lowest-frequency subpeak. Since this strong intensity transfer is not expected from Eq. (3.1), there should be some discrepancies between the measured data and Eq. (3.1) for temperatures above 400 K.

Figure 2 shows (a) the fitting result of the intensity of the $A_1(1TO)$ mode at 300 K and (b) the temperature dependence of the relative intensity of the lowest-frequency subpeak ($n=3$ to $n=4$) to the first subpeak ($n=0$ to $n=1$). Each subpeak was assumed to have an independent Lorentzian line shape. It is clear from Fig. 2(a) that the $A_1(1TO)$ peak consists of four distinct subpeaks. The complex line shape purely originates from the $A_1(1TO)$ mode, except for the

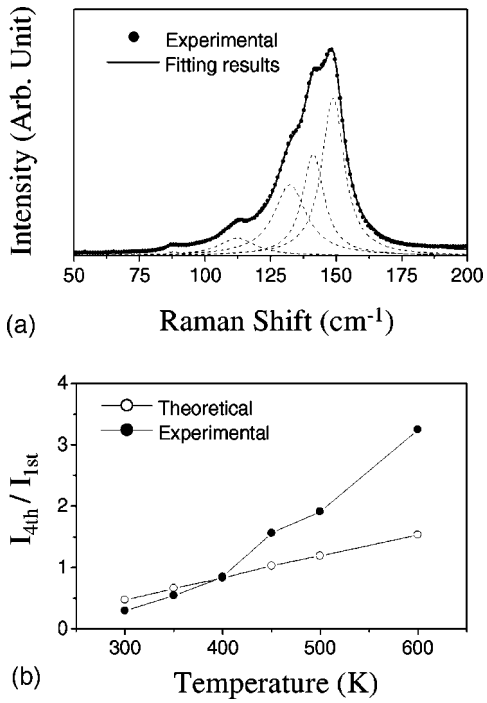

FIG. 2. The fitting result of the $A_1(1\mathrm{TO})$ mode: (a) the result of peak separation at 300 K, assuming that each subpeak has an independent Lorentzian shape, and (b) the temperature dependence of the relative intensity of the lowest-frequency subpeak to the first subpeak.

leakage of the strong $E(1\mathrm{TO})$ mode at 87.5 cm^{-1}. The major subpeak of the $A_1(1\mathrm{TO})$ mode at 300 K is the first subpeak. The fitting result also shows a significant line broadening with increasing quantum number. This reflects that the high-lying phonon states should have shorter lifetimes so that the peak line widths broaden gradually as the vibrational energy levels increase.

Figure 2(b) shows the temperature dependence of the relative intensity of the lowest-frequency subpeak to the first subpeak. The filled circles correspond to the values estimated from the measured spectra while the open circles represent the theoretically estimated ratios using Eq. (3.1). Beginning at 400 K, the experimentally obtained ratios deviate significantly from the theoretical values, and the degree of the deviation increases with increasing temperature.

One can extract a useful conclusion by deriving Eq. (3.1) and by reexamining the discrepancy between the experimental intensity ratios and the theoretical values in terms of this equation. According to the Fermi's golden rule, the rate of transition from a state ''n'' to another quantum state ''m'' (per unit time and volume) is given by the following well-known relation:

$$W_{nm}=\frac{2\pi}{\hbar}|\langle m|H'|n\rangle|^2\delta(E_m-E_n-\hbar\omega), \tag{3.2}$$

where H' is the perturbed Hamiltonian that induces a transition. The perturbed Hamiltonian for a charged particle (with charge e) caused by an external electromagnetic field can further be written as[23] $H'=ie\hbar/m\mathbf{A}\cdot\nabla$, where $\mathbf{A}$ is the vector potential. Now, the matrix element can be expanded using this expression of H'.

$$\begin{aligned}\langle m|H'|n\rangle &= -\sqrt{\frac{\hbar}{2\omega\epsilon}}\frac{d}{dt}\{\langle m|eq|n\rangle\}\\ &= i\sqrt{\frac{\hbar\omega}{2\epsilon}}\langle m|eq|n\rangle\\ &\equiv i\sqrt{\frac{\hbar\omega}{2\epsilon}}\mu_{nm},\end{aligned} \tag{3.3}$$

where ϵ is the dielectric permittivity of a medium, ω is the angular frequency of the external field, q is the time-dependent displacement of a charged element from its equilibrium position, and μ_{nm} denotes the transition dipole-moment integral for the $n\rightarrow m$ transition. In the derivation of the third expression of Eq. (3.3), we have used the Schrödinger picture[23] and the selection rule of harmonic transition (i.e., $\Delta n=1$). The term, $\langle m|q|n\rangle$, appearing in Eq. (3.3) can now be evaluated using the normalized eigenfunction for a linear harmonic oscillator, namely,

$$\begin{aligned}&\psi_n(q)=\left[\left(\frac{\alpha}{\pi}\right)^{1/2}\left(\frac{1}{2^n n!}\right)\right]^{1/2}\exp\left(\frac{-\alpha q^2}{2}\right)H_n(\sqrt{\alpha}q)\\ &\text{with}\quad \alpha=\left(\frac{m\omega}{\hbar}\right),\end{aligned} \tag{3.4}$$

where H_n is the nth-order Hermite polynomial. Thus, using Eq. (3.4) the matrix element can be compactly represented by the Kronecker δ_{ij}, namely,

$$\begin{aligned}\langle m|q|n\rangle &= \sqrt{\frac{\hbar}{2m\omega}}(\delta_{m,n-1}\sqrt{n}+\delta_{m,n+1}\sqrt{n+1})\\ &= \sqrt{\frac{\hbar}{2m\omega}}(n+1)^{1/2}.\end{aligned} \tag{3.5}$$

The last equality of Eq. (3.5) holds only for the $n\rightarrow n+1$ transition.

On the other hand, the δ function expression in Eq. (3.2) is proportional to the density of the initial quantum state and, thus, is proportional to $\exp(-E_n/k_BT)/Q_{vib}$, where Q_{vib} is the vibrational partition function. The intensity of a given transition is proportional to the population of the initial state. Thus, combining the expression for the density of the initial state with Eq. (3.5) for the $n\rightarrow n+1$ transition, one can immediately obtain the following expression for the ratio R from Eq. (3.2),

$$R=\left[\frac{\exp(-E_n/k_BT)}{\exp(-E_0/k_BT)}\right]\frac{|\langle n+1|q|n\rangle|^2}{|\langle 1|q|0\rangle|^2}=(n+1)\exp\left(\frac{-n\hbar\omega}{k_BT}\right). \tag{3.6}$$

The last equality holds only for the linear harmonic oscillator. Therefore, Eq. (3.1) is valid for a model based on the harmonic oscillator. It should be emphasized that the term

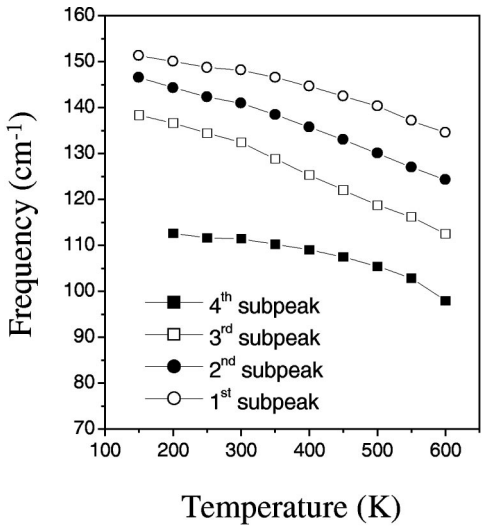

FIG. 3. The temperature dependence of subpeak frequencies of the A_1(1TO) mode of the undoped $PbTiO_3$ single crystal, showing the softening behavior with increasing temperature.

$(n+1)$ comes from the transition moment integral whereas the exponential term is stemmed from the density of the initial vibrational state.

As mentioned previously, Foster and co-workers[9,10] used Eq. (3.1) to test their anharmonicity model for the lowest-frequency A_1(1TO) phonon. However, it is now clear that this is self-contradictory. A quantitative agreement between the experimentally obtained intensity and the theoretical prediction for temperatures below 400 K, as they claimed, now indicates that it is not necessary to invoke the anharmonity effect to explain the observed relative intensity R of the A_1(1TO) mode for temperatures below 400 K. Contrary to the low-temperature behavior of the A_1(1TO) phonon, as summarized in Fig. 2(b), the observed strong intensity transfer toward the lowest-frequency subpeak for temperatures above 400 K cannot be properly explained by Eq. (3.1). Therefore, the anharmonicity effect might be the cause of the observed anomalous behavior of the A_1(1TO) phonon for temperatures above 400 K. We will systematically examine this important point in the following section.

B. Test of the anharmonicity model

In this section, we are going to present interesting experimental data for the A_1(1TO) mode before we will systematically analyze and test the anharmonicity model. Figure 3 shows the temperature dependence of subpeak frequencies of the A_1(1TO) mode. Although the frequencies of all four subpeaks show a softening behavior with increasing temperature, some differences in the slope of the softening are evident. The most unusual behavior is observed in the lowest-frequency subpeak that governs the high-temperature behavior of the A_1(1TO) phonon (Fig. 1). As shown in Fig. 3, while all other spacings between the subpeaks slightly increase with temperature, the spacing between the fourth (lowest frequency) and the third subpeak decreases with temperature.

The frequency of each subpeak is the transition energy between two corresponding quantum states. Therefore, the spacing between subpeak frequencies is the difference in their transition energies. This splitting seems to be caused by the anharmonicity of vibration. In case of the harmonic oscillator, there is no difference in the vibrational transition energy, and, thus, all subpeaks should merge into a single peak.

We will examine the anharmonicity model using the data presented in Fig. 3, in conjunction with the time-independent perturbation theory. According to the second-order perturbation theory, the eigenvalue of an anharmonic oscillator is given by

$$E_n = E_n^o + \langle \psi_n^o | H' | \psi_n^o \rangle + \sum_{n \neq m} \frac{|\langle \psi_m^o | H' | \psi_n^o \rangle|^2}{E_m^o - E_n^o}, \quad (3.7)$$

where ψ_n^o is the normalized unperturbed eigenfunction for a linear harmonic oscillator. The first term on the right-hand side of Eq. (3.7) corresponds to the harmonic approximation, whereas the second and the third terms respectively represent the first-order perturbation and the second-order correction to the energy eigenvalue.

In the ferroelectric state, the A_1(1TO) mode of $PbTiO_3$-type perovskites is naturally characterized by a double-well potential along the [001] direction. Then, in view of the Landau theory, the potential energy along this normal coordinate can be expressed using the order-parameter expansion, namely:[10,24]

$$\Phi(q') = -\frac{k}{2}q'^2 - \frac{\xi}{4}q'^4 + \frac{\zeta}{6}q'^6 + \cdots, \quad (3.8)$$

where q' is the displacement from the paraelectric cubic symmetry along the normal mode coordinate A_1 and all three coefficients, k, ξ, and ζ, have positive values. The negative sign appearing in the q'^4 term signifies the fact that $PbTiO_3$ has a discontinuous (first order) transition character. To apply the above expansion to the intrawell vibration that is relevant to the present discussion, it is necessary to move the origin of $\Phi(q')$ to one of the two minima in the double-well potential. After a tedious transformation procedure, one can obtain the following expression for the potential energy $\Phi(q)$ with its origin at one of the two minima in the double-well potential,

$$\begin{aligned}\Phi(q) &= (k\alpha - \zeta\alpha^5 + \xi\alpha)q + \left(-\frac{1}{2}k + \frac{5}{2}\zeta\alpha^4 - \frac{3}{2}\xi\alpha^2\right)q^2 \\ &\quad + \left(-\frac{10}{3}\zeta\alpha^3 + \xi\alpha\right)q^3 + \left(\frac{1}{4}\xi + \frac{5}{2}\zeta\alpha^2\right)q^4 \\ &\quad - \zeta\alpha q^5 + \frac{1}{6}\zeta q^6 + \cdots \\ &= aq + bq^2 + cq^3 + dq^4 + eq^5 + fq^6 + \cdots, \end{aligned} \quad (3.9)$$

where

$$\alpha^2 \equiv \frac{\xi + \sqrt{\xi^2 + 4k\zeta}}{2\zeta},$$

where q is the displacement from the minimum of double-well potential. One can readily show that the coefficients, b and d, have positive values. These changes in the sign of quadratic (harmonic) and quartic coefficients reflect the shift of the origin to the minimum of double-well potential. It is worth noting that the coefficients, a, c, and e, which are forbidden due to the symmetry [Eq. (3.8)], now appear in $\Phi(q)$. To assess the effect of anharmonic interatomic potential to the energy eigenvalue, we have taken the terms up to the quartic term in Eq. (3.9) and applied this potential to the second-order perturbation equation, Eq. (3.7). In this case, the Hamiltonian operator now reads,

$$H = H_o + H', \tag{3.10}$$

where

$$H_o = -\frac{\hbar^2}{2m}\frac{\partial^2}{\partial q^2} + bq^2, \quad \text{and} \quad H' = aq + cq^3 + dq^4.$$

The aq term in the perturbed Hamiltonian only yields the shift of the zero-point energy[25] and thus does not affect the subpeak frequency. Therefore, we will not consider this term any further. The first-order perturbation correction of the cq^3 term to the eigenvalue would be zero because of the oddness of the integrand. However, this term contributes to the energy eigenvalue through the second-order perturbation correction, namely,

$$\Delta E_n(cq^3) = c^2 \sum_{n \neq m} \frac{|\langle \psi_m^o | q^3 | \psi_n^o \rangle|^2}{E_m^o - E_n^o}. \tag{3.11}$$

One can evaluate this contribution[25] using the unperturbed eigenfunction given in Eq. (3.4), and the second-order correction is

$$\Delta E_n(cq^3) = -\frac{c^2}{8}\left(\frac{\hbar^2}{m^3\omega_o^4}\right)(30n^2 + 30n + 11). \tag{3.12}$$

Thus, the cubic term always reduces the energy eigenvalue regardless of the sign of the coefficient, c.

The dq^4 term affects the energy eigenstate only through the first-order correction, and the second-order correction always becomes zero because of the characteristic properties of the Hermite polynomial or the integrand. Therefore, we have

$$\Delta E_n(dq^4) = d\langle \psi_n^o | q^4 | \psi_n^o \rangle. \tag{3.13}$$

One can readily evaluate this contribution[26] using the eigenfunction presented in Eq. (3.4), and it is given by the following relation:

$$\Delta E_n(dq^4) = \frac{3}{4}d\left(\frac{\hbar}{m\omega_o}\right)^2(2n^2 + 2n + 1). \tag{3.14}$$

Since d is always positive, the quartic term (dq^4) always raises the energy eigenvalue of the intrawell vibration.

Considering the perturbation corrections ($cq^3 + dq^4$) up to second order, one can now obtain the net variation of the energy eigenvalue with respect to the eigenvalue of the unperturbed harmonic oscillator, and it is given by the sum of Eqs. (3.12) and (3.14).

$$\begin{aligned}\Delta E_n &= -\frac{c^2}{8}\left(\frac{\hbar^2}{m^3\omega_o^4}\right)(30n^2 + 30n + 11) \\ &\quad + \frac{3d}{4}\left(\frac{\hbar}{m\omega_o}\right)^2(2n^2 + 2n + 1) \\ &= \frac{\hbar^2}{4m^2\omega_o^2}\left(6d - 15\frac{c^2}{m\omega_o^2}\right)n(n+1) + \text{const.}\end{aligned} \tag{3.15}$$

Thus, the net difference in the energy eigenvalues between the nth and the $(n-1)$th quantum state and the corresponding subpeak frequency (ω_n) are given by the following relation:

$$\begin{aligned}E_n - E_{n-1} &= (E_n^o + \Delta E_n) - (E_{n-1}^o + \Delta E_{n-1}) \\ &= \hbar\omega_o - \frac{\hbar^2}{2m^2\omega_o^2}\left(15\frac{c^2}{m\omega_o^2} - 6d\right)n \\ &\equiv \hbar\omega_n.\end{aligned} \tag{3.16}$$

Comparing Eq. (3.16) with the experimental data presented in Fig. 3, one can immediately realize that $15c^2/m\omega_o^2 > 6d$. This signifies that the second-order perturbation correction of the cq^3 term is larger than the first-order correction of the dq^4 term to the energy eigenvalue.

The difference in the subpeak frequency between two adjacent vibrational quantum states is independent of the vibrational quantum number and is given by

$$\hbar\omega_n - \hbar\omega_{n+1} = \frac{\hbar^2}{2m^2\omega_o^2}\left(15\frac{c^2}{m\omega_o^2} - 6d\right) > 0. \tag{3.17}$$

Let us now consider the temperature dependence of the difference in the subpeak frequency. Among the three terms (c, d, ω_o) appeared in Eq. (3.17), ω_o is expected to have the most pronounced temperature dependence. As temperature approaches the phase-transition point, the harmonic frequency decreases substantially (phonon softening). This leads to the increase in the spacing between the subpeak frequencies with increasing temperature.

Therefore, if all of the subpeaks of the A_1(1TO) mode were purely originated from the anharmonicity of the intrawell vibration, all the spacings between adjacent subpeaks would increase with temperature. Contrary to this expectation, the spacing between the third subpeak and the lowest-frequency fourth subpeak decreases with increasing temperature, as is evident from Fig. 3. This observation obviously conflicts with the anharmonicity model described above. On the other hand, except for the lowest-frequency fourth subpeak, the spacings between two adjacent subpeaks are similar in their magnitudes at a given temperature but increase slightly with increasing temperature. This observation (Fig.

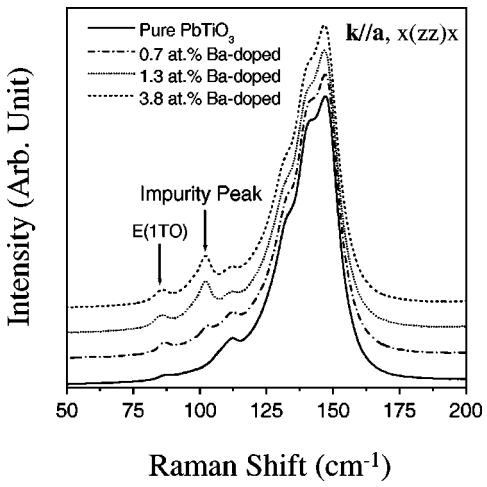

FIG. 4. Polarized Raman spectra of the $A_1(1TO)$ mode of pure and Ba-doped $PbTiO_3$ crystals at room temperature.

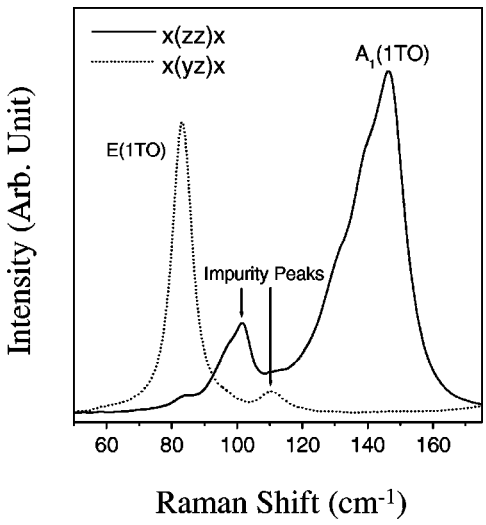

FIG. 5. The polarization dependence of the Ba-impurity peak. The spectrum marked with a solid line was obtained in $x(zz)x$ scattering geometry while the spectrum denoted by a dashed line was obtained in $x(yz)x$ scattering geometry.

3) clearly indicates that, except for the lowest-frequency subpeak, the splittings into several subpeaks are caused by the anharmonicity of the $A_1(1TO)$ mode. However, as extensively discussed in this section, the lowest-frequency subpeak (fourth subpeak) that dominates the high-temperature behavior of the $A_1(1TO)$ phonon is not originated from the anharmonicity of the normal A_1-mode vibration. We, therefore, will use a new independent labeling for the lowest-frequency subpeak and name it Q subpeak.

C. $A_1(1TO)$ mode of Ba-doped crystals

We are now in a position to seek the origin of the anomalous increase in the intensity of the lowest-frequency subpeak (Q subpeak) with increasing temperature. For this purpose, we have carefully compared the A_1-symmetry impurity peak of Ba-doped $PbTiO_3$ crystals with the Q subpeak of the $A_1(1TO)$ mode of pure $PbTiO_3$.

Figure 4 shows the polarized Raman spectra of the $A_1(1TO)$ mode of Ba-doped $PbTiO_3$ crystals having various contents of barium at room temperature. All the spectra were obtained in backscattering geometry with $x(zz)x$ polarization. The two outstanding features of Fig. 4 are the appearance of a new peak at near 100 cm^{-1} and the increase of its intensity with the Ba content. Since this peak is essentially absent in the pure, undoped $PbTiO_3$, it is considered as a Ba-impurity peak. A careful examination of the spectrum for the 3.8 at. % Ba-doped crystal further suggests that the Ba-impurity peak has a subpeak structure, which implies a possible existence of the anharmonicity in the vibration of the Ba-impurity mode.

Figure 5 shows the effect of the polarization condition of scattering on the Raman spectrum. According to the selection rules of Raman scattering, the active modes of the $x(zz)x$ scattering geometry are the A_1-symmetry phonons while those of the $x(yz)x$ scattering geometry are the E-symmetry phonons. The two peaks appearing in Fig. 5 are the $A_1(1TO)$ and E(1TO) modes. These two ''soft'' phonons have the lowest frequency in each corresponding symmetry and drive the ferroelectric phase transition. The eigenvectors of these modes are the relative displacements of the BO_6 octahedron with respect to the A-site ions (Pb^{2+}).[17] Therefore, these two phonons basically do not accompany the distortion of the BO_6 octahedron and have weak effective force constants, eventually leading to a phonon softening near the transition point.

As presented in Fig. 5, the Ba-impurity peak located near 100 cm^{-1} is visible only in the scattering geometry of the A_1 symmetry but is invisible in the scattering geometry of the E symmetry. This tells us the very important fact that normal mode associated with the Ba-impurity peak has the A_1 symmetry of the $PbTiO_3$ host lattice. In the scattering geometry of the E symmetry, another Ba-impurity peak is visible at near 110 cm^{-1}. However, this peak did not show any noticeable variation with temperature and, thus, is not believed to play any significant role in the soft-mode transition.

Figure 6 shows the temperature dependence of the frequency of the Ba-impurity peak having the A_1 symmetry of the host lattice. The Ba-content of the crystal was 3.8 at. %. As mentioned previously, the impurity peak has a subpeak structure. It has been decomposed into two distinct peaks, namely, the impurity peak 1 and the impurity peak 2, assuming that each individual subpeak has an independent Lorentzian line shape. As temperature increases, the frequencies of both subpeaks monotonously decrease, showing a typical softening behavior.[27] This suggests that the A_1-symmetry Ba-impurity peak is closely related to the soft-mode transition.

The temperature-dependent line shape of the $A_1(1TO)$ mode of the 3.8 at. % Ba-doped $PbTiO_3$ crystal is presented in Fig. 7. All the spectra were normalized with their integrated peak areas. All of the subpeaks move toward a low-frequency region with increasing temperature. The most conspicuous feature is the remarkable increase in the intensity of the Ba-impurity peak having the A_1 symmetry of the host

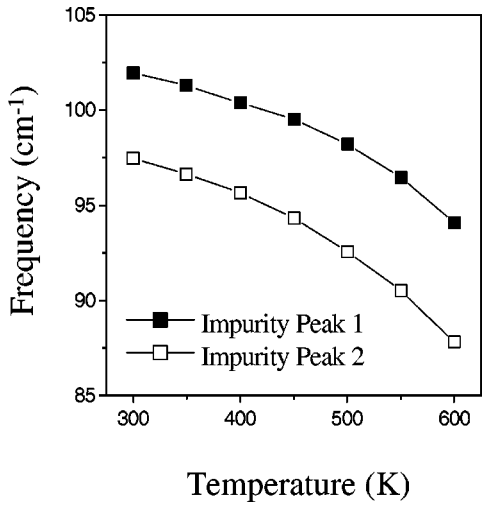

FIG. 6. The temperature-dependent subpeak frequencies of the Ba-impurity peak of the 3.8 at. % Ba-doped $PbTiO_3$ single crystal. The Ba-impurity peak was decomposed into two independent subpeaks.

lattice with increasing temperature. As shown in Fig. 7, this impurity peak completely governs the high-temperature behavior of the A_1(1TO) mode.

D. Origin of Ba-impurity mode

We have shown that the addition of barium to the pure $PbTiO_3$ crystal brings on the appearance of the A_1-symmetry impurity peak near 100 cm^{-1} and the behavior of this impurity peak is very similar to that of the Q subpeak of the A_1(1TO) mode of the undoped $PbTiO_3$. In this section, we will discuss possible origins of the Ba-impurity peak by systematically examining the characteristics of this impurity peak. The following three distinct mechanisms were considered as possible origins of the Ba-impurity peak: (i) high-order multiple phonon scattering caused by the variation of the phonon dispersion relation arising from the addition of Ba dopant, (ii) coupling of the A_1(TO) mode with another normal mode, and (iii) manifestation of a localized impurity mode which is directly influenced by the presence of Ba impurity.

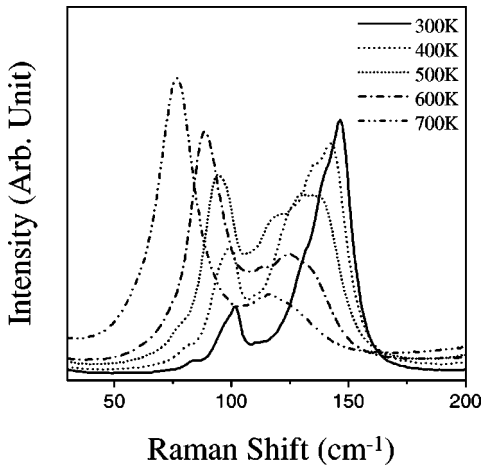

FIG. 7. The temperature dependence of Raman spectra for the A_1(1TO) mode of the 3.8 at. % Ba-doped $PbTiO_3$ single crystal.

Let us first consider the multiphonon scattering as a possible origin of the Ba-impurity peak near 100 cm^{-1}. Because of the similarity between the Ba-impurity peak and the Q subpeak, the multiple phonon scattering might be also important to understand the origin of the Q subpeak in the undoped $PbTiO_3$. Thus, the following discussion can be applied to the Q subpeak of the A_1(1TO) mode as well as the Ba-impurity peak. The multiple phonon scattering is not caused by the phonons located at the Brillouin zone center but is originated from the phonons having high density of states located at a certain singularity point within a phonon band. If two particular phonons are directly involved in the scattering process and their symmetric properties are, respectively, represented by Γ_1 and Γ_2 irreducible representations, then this two-phonon scattering process should follow the symmetry represented by $\Gamma_1 \otimes \Gamma_2$.[28]

It is important to notice that the impurity peak caused by the addition of barium follows the A_1 symmetry of the $PbTiO_3$ host lattice (Fig. 5). In C_{4v} point group, we have only three cases that give rise to the A_1 symmetry by the direct product of any two irreducible representations, and they are $A_1 \otimes A_1$, $B_1 \otimes B_1$, and $B_2 \otimes B_2$.[29] Because the normal mode vibration of $PbTiO_3$-type ferroelectric perovskites is described by $4A_1+B_1+5E$ irreducible representations (including three acoustic modes) and the conversion of the paraelectric T_{2u} mode into the B_1+E mode has not been observed (''silent'' mode) upon the transition to ferroelectric state, all the phonons involved in the multiple scattering should possess the A_1 symmetry if this multiphonon scattering is described by the overall A_1 symmetry. Although this symmetry requirement does not completely exclude an actual occurrence of the multiphonon scattering but reduces its possibility to a considerable degree.

The second point to be considered in the multiphonon scattering is the degree of peak broadening in the spectrum. In general, the degree of peak broadening in the multiple scattering is greater than that of the first-order scattering because more than one phonon is involved in the former. Contrary to this expectation, for both the Ba-impurity peak and the Q subpeak of the A_1(1TO) mode the values of the full width at half maximum (FWHM) are less than 10 cm^{-1}, which is comparable to or even smaller than the FWHMs of the first-order scattering peaks having the same A_1 symmetry.

Finally, we have considered the temperature-dependent scattering intensity. The temperature dependence of Raman-peak intensity for the multiple-phonon scattering is, in general, greater than that for the first-order scattering because more than one phonon participate in the multiple scattering and their relative distributions are sensitive to the variation of temperature.[30] Therefore, the temperature dependence of the peak intensity can be used as a useful criterion to judge whether a particular peak is a consequence of the multiple scattering or not. As presented in Figs. 5 and 6, the Ba-impurity peak has a subpeak structure, and, thus, it is difficult to precisely analyze its temperature dependence. Consid-

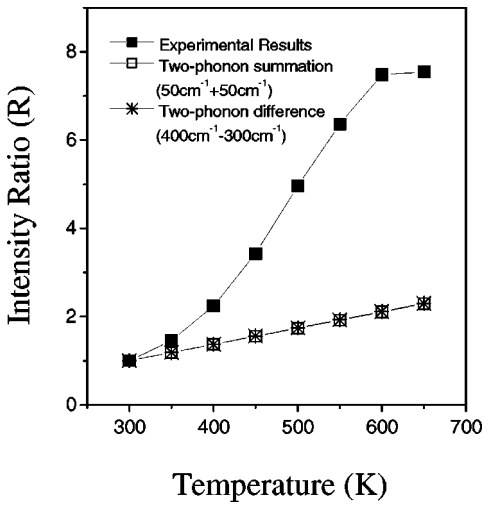

FIG. 8. The temperature-dependent relative intensity R of the lowest-frequency subpeak of the A_1(1TO) phonon with respect to the A_1(2TO) phonon. Open squares and asterisks denote the theoretically computed results assuming that the subpeak is originated from the two-phonon scattering process.

ering this difficulty, we carefully analyzed the temperature-dependent peak intensity of the Q subpeak of the A_1(1TO) mode, instead of the Ba-impurity peak, and subsequently judged the validity of the multiple-phonon scattering as a possible origin of the Ba-impurity peak. As discussed previously, the temperature dependence of the peak intensity for the Ba-impurity peak is very similar to that for the Q subpeak and both peaks originate from the normal modes having the same A_1 symmetry. Therefore, our conclusion deduced from the analysis of the Q subpeak can also be applied to the temperature dependence of the Ba-impurity peak.

Figure 8 compares the temperature dependence of the theoretically expected relative intensity ratio R for a hypothetically assumed two-phonon process with the experimentally obtained intensity ratio for the Q subpeak of the A_1(1TO) mode. The experimental data were obtained from the undoped, pure $PbTiO_3$ single crystal using $x(yy)x$ scattering geometry. The intensity of the A_1(2TO) mode was used as a reference for analyzing the temperature dependence of the Q-subpeak intensity. The intensity ratio R is defined as

$$R \equiv \frac{I_{Q-subpeak}(T)/I_{A_1(2TO)}(T)}{I_{Q-subpeak}(300K)/I_{A_1(2TO)}(300K)} = \frac{TF_{Q-subpeak}(T)/TF_{Q-subpeak}(300K)}{TF_{A_1(2TO)}(T)/TF_{A_1(2TO)}(300K)}, \quad (3.18)$$

where TF denotes the thermal factor. Assuming that the thermal factor is primarily determined by the phonon-distribution factor, the thermal factor for the Stoke line in the two-phonon process can be approximated as[30]

$$[n(\omega_1)+1][n(\omega_2)+1] \quad \text{for two-phonon summation}$$

$$[n(\omega_1)+1]n(\omega_2) \quad \text{for two-phonon difference}, \quad (3.19)$$

where

$$n(\omega) = \frac{1}{\exp\left(\frac{\hbar\omega}{k_B T}\right) - 1}.$$

We considered two possibilities that equally would give a peak at 100 cm^{-1}: two-phonon summation with 50 cm^{-1} $+50$ cm^{-1}, and two-phonon difference with 400 cm^{-1} -300 cm^{-1}. As shown in Fig. 8, the two distinct processes yield essentially the same temperature dependence. The most remarkable feature of Fig. 8 is that the intensity ratio of the Q subpeak of the A_1(1TO) mode exhibits a strong temperature dependence, which rules out the multiphonon scattering as a possible origin of the anomalous Q subpeak. This argument can equally be applied to the Ba-impurity peak that exhibits a similar temperature dependence. Therefore, it is highly unlikely that the appearance of the Ba-impurity peak at 100 cm^{-1} is a consequence of the multiple-phonon scattering.

As mentioned previously, another possible origin of the Ba-impurity peak is the coupling of the A_1(TO) mode with another normal mode. The mode-coupling model was suggested to explain the observed intensity transfer and the repulsion of Raman peaks in complex perovskites such as $Pb(Ti_{1-x}Zr_x)O_3$ (PZT) and $(Pb_{1-3/2x}La_x)TiO_3$ (PLT).[31–34] Among these studies, the observation made by Burns and Dacol[31] in the E symmetry of single-crystal $PbTi_{0.81}Sn_{0.19}O_3$ is notable and is similar, to a certain degree, to the results of the present study. However, there is a couple of important differences between these two. First, there is no sign of the repulsion between the subpeaks in the present case. Secondly, the frequency range of the anomalous Q subpeak or the Ba-impurity peak is substantially higher than that of the E mode studied by Burns and Dacol. According to the mode-coupling model, the coupling of a zone-center soft mode to a zone-boundary transverse acoustic (TA) mode is most probable in $PbTiO_3$-based perovskites. The neutron-scattering study showed that the frequency range of the TA mode in $PbTiO_3$ was sufficiently below 80 cm^{-1} and is even below the frequency of the E(1TO) mode.[35] Moreover, the phonon dispersion curve tells us that there does not exist any phonon band that possibly couples to the A_1(1TO) mode for the frequency range between the A_1(1TO) mode and E(1TO) mode.[17] In view of these, the Q subpeak or the Ba-impurity peak cannot be attributed to the mode coupling.

The last possibility to be considered as the origin of the observed Ba-impurity peak is the A_1-symmetry localized mode directly influenced by the Ba dopant. This localized mode can be viewed as a modified A_1(1TO) mode by the effect of Ba-impurity ions. More specifically, both the localized Ba-impurity mode with the A_1 symmetry and the A_1(1TO) mode in the pure $PbTiO_3$ have the same eigenvector for the relative atomic displacement. The main difference between these two modes is the vibration frequency or the effective force constant. The A_1(1TO) mode within a certain correlation radius (R_c) centered at a given impurity ion will be influenced by this Ba-impurity center. Then, the photons scattered from this region will build up an A_1-symmetry im-

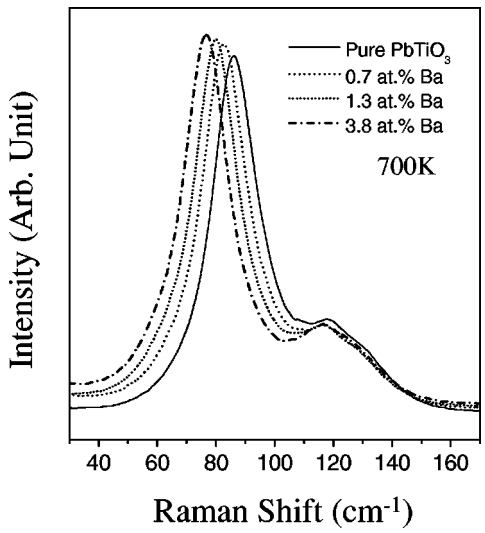

FIG. 9. The variation of the line shape of the $A_1(1TO)$ mode with the Ba content at 700 K.

purity peak. At a low temperature, the region influenced by the Ba-impurity center is confined to a small volume. However, the correlation radius of the localized region increases drastically as temperature approaches the phase-transition point. This Ba-impurity mode qualitatively explains all the observations, including the anomalous increase in the intensity of the Ba-impurity peak with temperature (Fig. 7). Considering all the discussion made in this section, we now conclude that the Ba-impurity mode is a localized transverse optic A_1-symmetry mode directly influenced by the Ba impurity and is primarily responsible for the existence and growth of the Ba-impurity peak near 100 cm^{-1}.

E. The lowest-frequency subpeak of $A_1(1TO)$ mode

Figure 9 shows the variation of the line shape of the $A_1(1TO)$ mode with the Ba content at 700 K. Regardless of the presence and the content of barium ions, all the spectra show similar line shapes. The only difference is the degree of the frequency shift in the major subpeak. Despite the distinct difference in the history of thermal evolution between the Ba-impurity peak and the Q subpeak of the $A_1(1TO)$ mode of the undoped $PbTiO_3$, both modes have very similar line shapes (Fig. 9) and show a gradual softening with temperature (Figs. 3 and 6). In addition to this, these two modes commonly share the A_1 symmetry in the relative atomic displacements. All these indicate that the physical origin of the Ba-impurity mode is essentially the same as that of the lowest-frequency Q subpeak of the $A_1(1TO)$ mode that governs the soft-mode transition.

Another important observation associated with the anomalous line shape of the $A_1(1TO)$ mode is that, in contrast with the undoped $PbTiO_3$ (Figs. 1 and 2), the Ba-doped crystals do not show any increase in the intensity of the Q subpeak. Instead, a strong intensity increase of the Ba-impurity mode was observed with increasing temperature (Fig. 7). This observation suggests that there is an intensity transfer from the Q subpeak of the $A_1(1TO)$ mode to the Ba-impurity mode by the Ba doping. In other words, the Q subpeak of the $A_1(1TO)$ mode is gradually replaced by the Ba-impurity mode with the Ba doping. If the lowest-frequency Q subpeak of the $A_1(1TO)$ mode had some intrinsic origins, this mode replacement could not be explained because all other subpeaks of the $A_1(1TO)$ mode that originated from the intrinsic lattice anharmonicity showed no significant change by the Ba doping (near 120 cm^{-1} in Fig. 9).

Above discussion clearly suggests that the anomalous line shape of the Q subpeak of the $A_1(1TO)$ mode also stems from some extrinsic origins. In other words, the Q subpeak of the $A_1(1TO)$ mode of the undoped $PbTiO_3$ is caused by some unavoidable defects. This model based on the lattice defects can explain all the observations, including (i) the anomalous increase in the intensity of the lowest-frequency subpeak (pure $PbTiO_3$) and the Ba-impurity mode with temperature and (ii) the mode replacement by the Ba doping.

Possible defects that can potentially cause the appearance of the Q subpeak are substitutional impurities or lattice defects such as vacancies. The ICP analysis of the undoped crystal indicated that the total content of impurities was less than 10 ppm in atomic fraction. The detected impurities were Ca, Co, Mg, Cr, P, and Cd. These impurity levels are negligible compared to the Ba content ($0.7 \sim 3.8$ at. %) employed in the present study. Therefore, substitutional impurities are not likely to be the origin of the anomalous line shape of the $A_1(1TO)$ mode. Another possible origin of the anomalous line shape is related to some unavoidable lattice defects. Thermodynamics tells us that these defects cannot be completely eliminated. The concentration of thermodynamically stable defects, in general, increases rapidly with temperature. In an ionic crystal like $PbTiO_3$, even a trace amount of charged lattice defects (e.g., vacancies) can affect the phonon modes through a long-range electrostatic interaction.

F. Correlation of local polarization fluctuations

One of the prominent features of the $A_1(1TO)$ mode is that its high-temperature line shape is governed by low-frequency subpeaks. This feature has been shown in the lowest-frequency Q subpeak of the undoped $PbTiO_3$ and in the Ba-impurity peak of the Ba-doped crystals. According to the discussion made in Secs. III D and III E, these subpeaks originate from some lattice defects (Q subpeak) or impurities (Ba-impurity peak). Considering low relative concentrations of these defects or impurities, however, the observed dominance is quite remarkable. The main purpose of this final section is to qualitatively address this important point.

It is expected that crystal defects would have influence on the behavior of the $A_1(1TO)$ mode either through an elastic path (in case of the Ba impurity) or through a long-range electrostatic path (in case of the charged lattice defects). These defect modes can be regarded as frozen fluctuations of order parameters or polarizations. At a low temperature, the local frozen fluctuations caused by these defects or impurities are confined to a very small region around the impurity center. As temperature increases, however, the correlation of these local polarizations (local order parameters) increases

sharply and the system is infinitely compliant to external perturbations at the critical point T_c. The best measure of the strength of this correlation is known as the correlation function ($G_{\alpha\beta}$) of the displacements of atoms from the average positions and can be written, in the coordinate representation, as[36]

$$G_{\alpha\beta}(\mathbf{x}) \equiv \frac{\langle q_\alpha(\mathbf{x}) q_\beta(0)\rangle}{k_B T} = \frac{\nu_0}{(2\pi)^3}\int G_{\alpha\beta}(\mathbf{k}) e^{ik\cdot x} d\mathbf{k} \approx l \frac{1}{|\mathbf{x}|}\exp\left(\frac{-|\mathbf{x}|}{R_c}\right), \tag{3.20}$$

where $q_\alpha(\mathbf{x})$ denotes the standard displacement coordinate for the αth degree of freedom at the spatial coordinate $\mathbf{x}$. It can be related to the ionic component of the spontaneous polarization by $P_\alpha = z/\nu_o \langle q_\alpha\rangle$, where ν_o is the volume of a crystal. $G_{\alpha\beta}(\mathbf{k})$ denotes the Fourier transform pair of $G_{\alpha\beta}(\mathbf{x})$, and l is an appropriate constant. Thus, for the A_1 symmetry of ABO_3-type perovskites, $q_\alpha(\mathbf{x})$ can be regarded as the displacement that is parallel to the relative displacement of the BO_6 octahedron with respect to the A-site ions. The last expression can be obtained by using the quasiharmonic approximation for a displacive transition.[36] The correlation radius R_c for $T<T_c$, can be written as

$$R_c = l' \sqrt{\frac{T_c}{T_c - T}}, \tag{3.21}$$

where l' is another proportionality constant. The above equation tells us that the correlation length becomes infinite as temperature approaches the critical point.

One important feature associated with the defect or impurity modes is that, at a given temperature, the frequencies of these modes are significantly lower than those of the intrinsic vibrations having the same A_1 symmetry. This unique feature remains unaffected up to 700 K. These are summarized in Fig. 1 for the lowest-frequency Q subpeak of the A_1(1TO) mode of the undoped $PbTiO_3$ and in Fig. 7 for the A_1-symmetry Ba-impurity mode of the Ba-doped crystals. All these results suggest that the local Curie point of the defected region would be significantly lower than that of the intrinsic region, which is free of the lattice defects or impurities. Thus, like a selective nucleation at heterogeneous sites, the polarization correlation selectively initiates at these defect or impurity sites. The correlation length increases drastically as temperature approaches the critical point that corresponds to the local region around the defect center, and the whole crystal will be under the influence of this long-range polarization correlation.

Now, we are in a position to address the following important question: Why do the defect (impurity) modes dominate the high-temperature behavior of the A_1(1TO) phonon that is primarily responsible for the soft-mode transition in ABO_3-type perovskites? The answer to this question is directly related to the fact that, over a wide range of temperature, the phonon frequencies of these defect modes are significantly lower than those of the corresponding intrinsic vibrations having the same A_1 symmetry.

IV. CONCLUSIONS

It is shown that the lowest-frequency Q subpeak of the A_1(1TO) mode that dominated the phonon softening of the undoped $PbTiO_3$ cannot be properly explained by the previously proposed anharmonicity model. The polarized Raman spectra of the A_1(1TO) mode of Ba-doped $PbTiO_3$ crystals showed that the Ba-impurity mode that dominated the soft-mode transition also had the A_1 symmetry of the $PbTiO_3$ host lattice. By carefully comparing the impurity peak of the Ba-doped crystals with the lowest-frequency Q subpeak of the A_1(1TO) mode of the undoped $PbTiO_3$, we have concluded that the anomalous line shape of the A_1(1TO) phonon is caused not only by the lattice anharmonicity but also by some lattice defects. Particularly, the lowest-frequency subpeak of the A_1(1TO) mode is not directly related to the anharmonicity but presumably originates from the existence of thermodynamically unavoidable lattice defects.

ACKNOWLEDGMENTS

This work was financially supported by the Korea Institute of Science and Technology Evaluation and Planning (KISTEP) through the NRL program and by the Korea Research Foundation (KRF), under Contract No. E01779, 1999.

*Email address: hmjang@postech.ac.kr

[1] G. Burns and B. A. Scott, Phys. Rev. B **7**, 3088 (1973).
[2] N. Sicron, B. Ravel, Y. Yacoby, E. A. Stern, F. Dogan, and J. J. Rher, Phys. Rev. B **50**, 13 168 (1994).
[3] M. D. Fontana, K. Wojcik, H. Idrissi, and G. E. Kugel, Ferroelectrics **107**, 91 (1990).
[4] Y. Girshberg and Y. Yacoby, Solid State Commun. **103**, 425 (1997).
[5] Y. Yacoby, Y. Girshberg, and E. A. Stern, Z. Phys. B: Condens. Matter **104**, 725 (1997).
[6] M. E. Lines and A. M. Glass, *Principles and Applications of Ferroelectrics and Related Materials* (Clarendon Press, Oxford, 1982).
[7] G. Burns and B. A. Scott, Phys. Rev. Lett. **25**, 167 (1970).
[8] M. D. Fontana, H. Idrissi, G. E. Kugel, and K. Wojcik, J. Phys.: Condens. Matter **3**, 8695 (1991).
[9] C. M. Foster, Z. Li, M. Grimsditch, S.-K. Chan, and D. J. Lam, Phys. Rev. B **48**, 10 160 (1993).
[10] C. M. Foster, M. Grimsditch, Z. Li, and V. G. Karpov, Phys. Rev. Lett. **71**, 1258 (1993).
[11] S. M. Cho and H. M. Jang, Appl. Phys. Lett. **76**, 3014 (2000).
[12] G. Shirane, J. D. Axe, and J. Harada, Phys. Rev. B **2**, 155 (1970).
[13] J. A. Sanjurjo, E. Lopez-Cruz, and G. Burns, Phys. Rev. B **28**, 7260 (1983).
[14] N. Takesue and H. Chen, J. Appl. Phys. **76**, 5856 (1994).
[15] J. Frantti and V. Lantto, Phys. Rev. B **54**, 12 139 (1996).
[16] J. Frantti and V. Lantto, Phys. Rev. B **56**, 221 (1997).
[17] J. D. Freire and R. S. Katiyar, Phys. Rev. B **37**, 2074 (1988).

[18] G. Burns, Phys. Rev. B **10**, 1951 (1974).
[19] A. Bussmann-Holder, H. Bilz, and G. Benedek, Phys. Rev. B **39**, 9214 (1989).
[20] J. Frantti, V. Lantto, S. Nishio, and M. Kakihana, Phys. Rev. B **59**, 12 (1999).
[21] J. C. Loulergue and J. Etchepare, Phys. Rev. B **52**, 15 160 (1995).
[22] X. H. Dai, Z. Li, X. Z. Xu, S.-K. Chan, and D. J. Lam, Ferroelectrics **135**, 39 (1992).
[23] See, for example, J. Singh, *Quantum Mechanics* (Wiley, New York, 1997), Chap. 9.
[24] T. Hidaka, J. Phys. Soc. Jpn. **61**, 1054 (1992).
[25] See, for example, C. Cohen-Tannoudji, B. Diu, and F. Laloe, *Quantum Mechanics* Vol. 1 (Herman/Wiley, Paris/New York, 1970), Chap. 11.
[26] See, for example, S. Wieder, *The Foundations of Quantum Theory* (Academic Press, Orlando, 1973), Chap. 7.
[27] W. Cochran, Adv. Phys. **9**, 387 (1960).
[28] R. A. Evarestov and V. P. Smirnov, *Site Symmetry in Crystals* (Springer-Verlag, New York, 1993), p. 214.
[29] E. B. Wilson, Jr., J. C. Decius, and P. C. Cross, *Molecular Vibrations* (Dover, New York, 1955), p. 331.
[30] W. Hayes and R. Loudon, *Scattering of Light by Crystals* (Wiley, New York, 1978), p. 92.
[31] G. Burns and F. H. Dacol, Solid State Commun. **18**, 1325 (1976).
[32] D. Bäuerle, Y. Yacoby, and W. Richter, Solid State Commun. **14**, 1137 (1974).
[33] R. Merlin, J. A. Sanjurjo, and A. Pinczuk, Solid State Commun. **16**, 931 (1975).
[34] G. Harbeke, E. F. Steigmeier, and R. K. Wehner, Solid State Commun. **8**, 1765 (1970).
[35] G. Shirane, J. D. Axe, J. Harada, and J. P. Remeika, Phys. Rev. B **2**, 155 (1970).
[36] G. A. Smolenskii *et al.*, in *Ferroelectrics and Related Materials*, edited by G. W. Taylor, Ferroelectricity and Related Phenomena, Vol. 3 (Gordon and Breach, New York, 1984), Chap. 5.